

Concept of a measurement and test station to determine linear pressure drop and the heat transfer coefficient of internally ribbed tubes

Karol Majewski*

Cracow University of Technology
Al. Jana Pawla II 37, 31-864 Krakow, Poland

Abstract

This paper presents applications for internally finned tubes in boilers designed for supercritical parameters. It outlines the characteristic dimensions of a tube used for the construction of a test station to determine the heat transfer coefficient and linear friction losses pertaining to flows inside internally ribbed tubes. Theoretical dependencies used for predicting the heat transfer coefficient and linear friction losses are presented herein. The paper ends with a description of the test station.

Keywords: Linear pressure drop, Heat transfer coefficient, Internally ribbed tube

1. Introduction

State-of-the-art technologies related to progress in the power engineering industry help to improve performance in terms of processes. Increasing working medium parameters in terms of pressure and temperature is one way to achieve improved efficiency. With a view to using the chemical energy of fuel in the most effective way, plants are designed with supercritical and ultra-supercritical parameters. Such solutions require the use of appropriate materials and design approaches. As far as power boilers are concerned, two design solutions in the scope of evaporators are predominant: spiral and vertical Benson Once-Through evaporators. For the latter type of tubing, depending on the boiler zone, ducts with various geometry are used. The most thermally loaded heating surfaces of the combustion chamber are made of finned tubing (internally ribbed tubing).

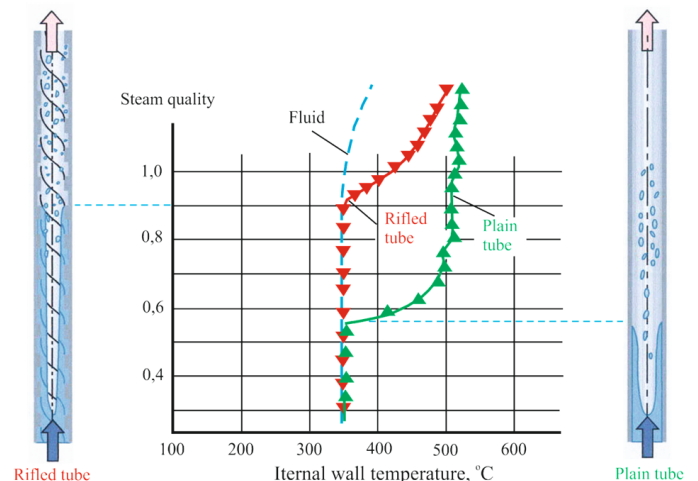


Figure 1: Comparison between evaporation zones and inner wall temperature in rifled and plain tubes

Internally ribbed tubing helps to decrease mass flow and ensures sufficient cooling for the internal surfaces of tubes. Moreover, the departure from nucleate boiling is shifted towards higher values of vapor quality, compared to plain tubing (Fig. 1).

Studies prepared by one boiler manufacturer show

*Corresponding author

Email address: kmajewski@mech.pk.edu.pl (Karol Majewski*)

Table 1: Chemical composition of 13CrMo44 steel [7–9]

Element	C	Si	Mn	Cr	Mo	Cu
Content, %	0.14	max. 0.40	0.55	0.98	0.60	max. 0.30

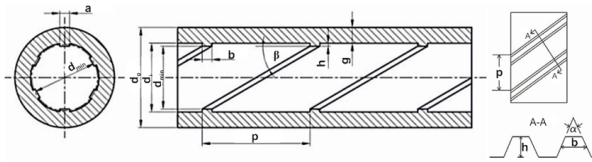


Figure 2: Rifled tube cross-section with characteristic dimensions

that evaporators containing internally ribbed tubing make it possible to lower the water wall mass and provide easy access to particular components during inspections and repairs. At the same time, optimized rib design helps to decrease pressure drop pertaining to medium flow [1–3].

Finned tubing was installed at a Polish power plant, in a 460 MW CFB boiler. It was deployed in the most thermally loaded boiler zones, i.e. within the wing walls. The temperature of the bed in this part of the boiler is approx. 900°C which, if plain tubing is used, may induce the phenomenon of film boiling [4–6]. The complex internal surface of tubing combined with changed heat exchange processes and flows require an understanding of new phenomena and the impact of geometry on the phenomena under investigation. Therefore, the concept of a measurement and test station has been developed to enable determination of the impact of internally ribbed tubing geometry on the heat transfer coefficient and linear friction losses.

2. Characteristic dimensions of ribbed tubing

For the purposes of measurement station construction, an internally ribbed tube made of 13CrMo44 steel will be used. This is a chrome-molybdenum steel used for the manufacture of pressure elements designed for operation in high-temperature environments. Chemical composition and selected material properties are shown in tables 1 and 2.

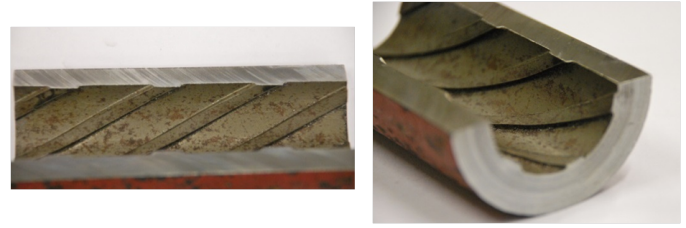


Figure 3: Rifled tube cross-section

Figure 2 presents the characteristic dimensions of the internally ribbed tube. Characteristic values pertaining to ribs result in changed flow and thermal conditions compared to plain tubing. Later in this study equations describing heat exchange and the impact of the above-mentioned geometry on pressure drop will be presented. Presented below are explanations of selected values and dimensions of the finned tube, which belongs to the Institute of Machines and Power Engineering Equipment of the Cracow University of Technology. Figure 3 shows a picture of the finned tube under investigation.

- d_o —outside diameter 50.8 mm
- d_i —inside diameter (without ribs) 34.9 mm
- d_{min} —minimum diameter 32.9 mm
- g —wall thickness 7.95 mm
- e —rib height 1 mm
- p —fin pitch 30 mm
- a —width of the rib (at base) 5 mm
- b —average rib width 4.5 mm
- α —included angle 45°
- β —helix angle 30°
- N —number of fin starts 6

3. Pressure drop examination

3.1. Determination of pressure drop in finned tubing

In general, unitary pressure drop pertaining to tubing flow is given by the expression:

Table 2: Selected properties of 13CrMo44 steel as a temperature function [10]

Temperature, °C	0	20	50	100	200	300	400	500	600
Density, kg/m ³	7855	7849	7840	7825	7793	7759	7724	7687	7648
Modulus of elasticity, MPa·10 ⁵	2.153	2.140	2.121	2.087	2.017	1.940	1.859	1.772	1.680
Thermal expansion, (1/K)·10 ⁻⁵	1.16	1.19	1.24	1.31	1.43	1.53	1.60	1.64	1.66
Thermal conductivity, W/(mK)	43.9	44.1	44.4	44.6	44.0	42.2	39.8	37.0	34.1
Specific heat, J/(kgK)	461	464	469	480	511	555	612	681	762

$$\left(\frac{\Delta p}{L}\right) = \left(\frac{\Delta p}{L}\right)_f + \left(\frac{\Delta p}{L}\right)_h + \left(\frac{\Delta p}{L}\right)_a \quad (1)$$

where: $\left(\frac{\Delta p}{L}\right)_f$ —pressure drop due to friction, $\left(\frac{\Delta p}{L}\right)_h$ —hydrostatic pressure losses, $\left(\frac{\Delta p}{L}\right)_a$ —losses due to impulse of force.

Losses related to height difference and impulse of force for flowing liquid are determined in similar fashion to the general case.

With respect to the internally ribbed tubing discussed here, loss related to friction is of the utmost importance. This is due to the complex internal surface of the duct and phenomena that take place extensively next to the wall. Unitary linear pressure drop is derived from the following equation:

$$\left(\frac{\Delta p}{L}\right)_f = 4f \cdot \frac{\rho v^2}{2d} \quad (2)$$

For plain tubing the linear loss coefficient directly depends on the Reynolds number. For laminar flow $Re < 2300$ the Hagen-Poiseuille equation is used:

$$f = \frac{16}{Re} \quad (3)$$

and for turbulent flows, the Blasius equation is used:

$$\begin{aligned} f &= \frac{0.079}{Re^{0.25}} & Re < 10^5 \\ f &= \frac{0.046}{Re^{0.2}} & Re > 10^5 \end{aligned} \quad (4)$$

In the case of internally ribbed tubing it is not possible to use traditional dependencies relating to

plain and rough tubing. This is due to the rib geometry and their helix angle. One of the correlations used for predicting linear losses was developed by Gregory Zdaniuk et al. [11], where it pertains to pressure drop in lower-diameter tubing fitted with more ribs. Experimental verification was carried out for the Reynolds number in the range of $12000 < Re < 60000$:

$$f = 0.128Re^{-0.305} N^{0.235} \left(\frac{e}{d_i}\right)^{0.319} \beta^{0.397} \quad (5)$$

Another equation was proposed by Ralph Webb et al. [12]. This team derived dependencies based on geometrical factors, similarly to Zdaniuk et al. The equation was developed based on water and cooling media flow examination:

$$f = 0.108Re^{-0.283} N^{0.221} \left(\frac{e}{d_i}\right)^{0.785} \beta^{0.78} \quad (6)$$

Jensen and Vlakancic in their study [13] refer to the linear losses coefficient formula derived by Carnavos:

$$f = 0.046Re^{-0.2} \left(\frac{A_n}{A_{xs}}\right)^{-0.5} (\sec\beta)^{0.75} \quad (7)$$

where: $A_n = 0.25\pi d_i^2$, m^2 —surface of cross-sectional profile (without ribs), $A_{xs} = A_n - N \cdot e \cdot b$, m^2 —actual flow cross-section.

Equations (3...7) involve linear losses coefficient formulas by Fanning. Dependency pertaining to coefficient of friction losses defined by Moody is often found in the literature on the subject. The following relation exists between the cited dependencies:

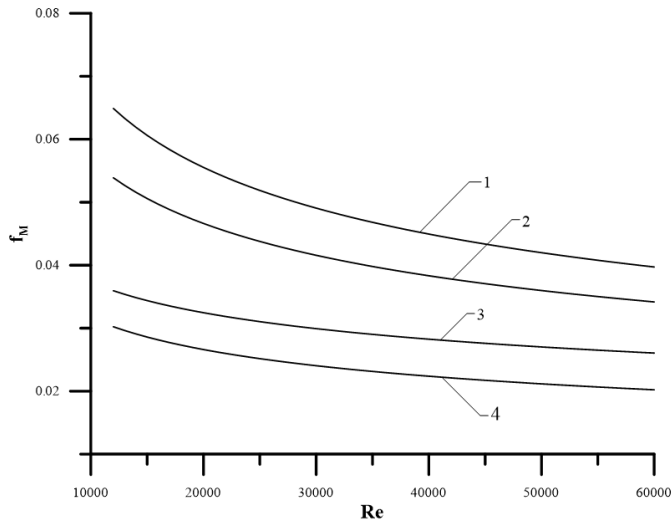


Figure 4: Comparison between Moody's friction factor in Reynolds number function: 1—Zdaniuk et al., 2—Webb et al., 3—Carnavos, 4—Blasius

$$f_M = 4f \quad (8)$$

The developed station will allow for verification of the cited equations (5...7) and determination of dependencies fitted for the presented geometry.

3.2. Numerical comparison of dependencies pertaining to pressure drop in finned tubing

As shown in chapter 3.1, determination of the linear pressure drop coefficient in finned tubing is based on parameters other than in the case of equations related to plain tubing. For comparison purposes, calculations using the following equations were carried out: (4) for plain tubing, and (5...7) for finned tubing. The Reynolds number in the range from 1.2×10^4 to 6×10^5 was used as the main comparison criteria. For calculation of the linear losses coefficient the following tubing was used: a finned tube with the geometry presented in section 2 and a plain tube of the same internal diameter d_i as in the case of internally ribbed tube. The results obtained are shown in Fig. 4.

Analysis shows that pressure drop pertaining to liquid flow for the identical Reynolds number is higher in the finned tubing (Fig. 4, curves 1...3) than in the plain tubing (Fig. 4, curve 4). The size of losses depends on the number of ribs, rib height-tubing internal diameter ratio, and helix angle.

4. Determination of heat transfer coefficient

Heat exchange occurs if the tubing wall temperature differs from the fluid temperature. Heat flux exchanged between the perfused solid body and fluid is defined by Newton's law [14]. Upon transformation of the dependency, a formula for calculation of the local heat transfer coefficient [5] is obtained:

$$h = \frac{\dot{q}}{T_w - T_b} \quad (9)$$

where: \dot{q} —heat flux, W/m^2 ; T_w —inner wall temperature, K; T_b —bulk temperature, K.

Equation (9) is a general purpose equation and can be used in the presented case. Another method for the determination of the convective heat transfer coefficient involves the use of Chilton-Colburn parameter j . This value is predicted based on the Reynolds number and the geometric dimensions of a duct. In a general case the Chilton-Colburn parameter is determined by means of an equation shown in studies [11–14]:

$$j = St \cdot Pr^{\frac{2}{3}} \quad (10)$$

Using the Stanton number definition [14] the convective heat transfer coefficient can be determined:

$$h = j c_p G \cdot Pr^{-\frac{2}{3}} \quad (11)$$

Webb et al. [12] determined the Chilton-Colburn parameter as:

$$j = 0.00933 Re^{-0.181} N^{0.285} \left(\frac{e}{d_i} \right)^{0.323} \beta^{0.505} \quad (12)$$

Whereas Zdaniuk and his team referred to equation (12) in their research and proposed the following dependency for calculation of parameter j [11]:

$$j = 0.029 Re^{-0.347} N^{0.253} \left(\frac{e}{d_i} \right)^{0.0877} \beta^{0.362} \quad (13)$$

Another method for determination of the convective heat transfer coefficient involves the use of a formula for calculation of the Nusselt number:

$$Nu = \frac{l_c h}{k} \quad (14)$$

where: l_c —characteristic length, m, h —convective heat transfer coefficient, W/(m²K), k —fluid thermal conductivity [W/(mK)].

With respect to this method, the specification of characteristic duct geometry is intricate. It requires specifying the shape function. One of the formulas for determination of the Nusselt number was proposed by Jensen and Vlakancic [13]:

$$\frac{Nu}{Nu_p} = \left(\frac{l_{csw}}{d_i} \right)^{-0.5} \left(\frac{A_n}{A_{xs}} \right)^{0.8} [f(\text{geometry})] \quad (15)$$

For the duct under investigation the coefficients used in equation (16) have the following values:

$$\frac{l_{csw}}{d_i} = [1 - A(SW)^b(H)^c(W)^d] \quad (16)$$

$$f(\text{geometry}) = \left(\frac{SA_{act}}{SA_n} \right)^{0.29} [1 - 1.792(SW)^{0.64}(H)^{2.76}(Re)^{0.27}] \quad (17)$$

For equations (16...17) the following values are used: $SW = N \sin\left(\frac{\beta}{\pi}\right)$ —dimensionless modified rib pitch, $H = \frac{2e}{d_i}$ —dimensionless rib height coefficient, $W = \left(\frac{\pi}{N} - \frac{e}{d_i}\right) \cos\beta$ —dimensionless coefficient of flow between ribs, SA_{act} —internal heat transfer area including rib surface area, SA —internal surface of plain pipe of diameter d_i .

5. Concept of the measurement station design

In order to determine the values presented in chapters 3 and 4 the measurement and test station concept has been developed. It will enable determination of linear pressure drop and the local heat transfer coefficient for the tubing described in chapter 2 herein. The station diagram is shown in Fig. 5.

Flows will be tested in vertically mounted tubing 3 m long. Plain tubing will also be used in order to allow for parameter comparison against finned tubing. The arrangement of measuring points for both types of tubing is shown in Fig. 6. The spacing between individual measuring points will be 0.5 m, resulting in 7 measuring points for the total ducting length. Individual values will be measured as follows, respectively:

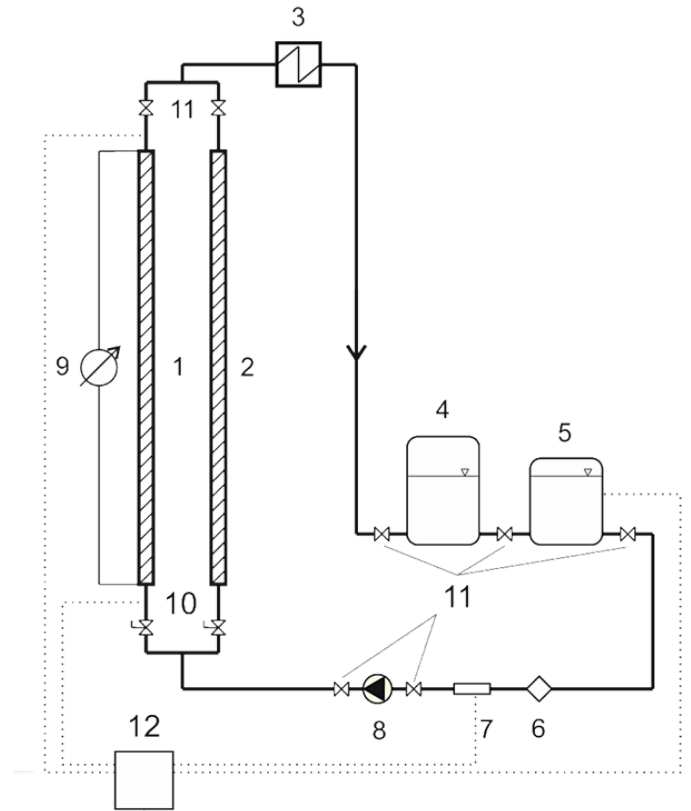


Figure 5: Concept of the measurement and test station: 1—rifled tube, 2—plain tube, 3—cooler, 4—feed water tank, 5—buffer water tank, 6—filter, 7—flowmeter, 8—pump, 9—transformer, 10—regulation valves, 11—cut-off valves, 12—data acquisition system

- internal wall temperature: 1...7
- fluid temperature: 1 and 7,
- pressure drop: between points 4 and 6.

For the purposes of measuring wall temperature on the internal surface, 5 thermocouples will be installed for each measuring point on the finned tubing (angle between thermocouples: $\gamma = 72^\circ$). This number of thermocouples will enable the averaging of tubing internal surface temperature. Temperature distribution for the plain tubing will be more uniform; thus, 2 thermocouples will be mounted opposite each other for each measuring point, where adjacent measuring points will be turned through an angle of 90° to each other.

In order to predict the local heat transfer coefficient, heaters will be deployed along the whole length of the tubing. The heat flux transferred by them will be

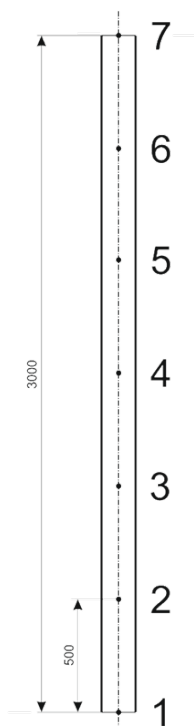


Figure 6: Measure points

measured and subsequently used for calculations. To limit the environmental impact, both finned and plain tubing will be thermally insulated.

Water will serve as a working medium. For the station under investigation the estimated fluid temperature range will be between ambient temperature (approx. 20°C) and near-boiling point at atmospheric pressure (approx. 90°C). The flux of the flowing medium will be measured by means of a flowmeter, presented in Fig. 5 (position no. 7).

6. Conclusions

The measurement station concept presented in chapter 5 will make it possible to determine the heat transfer coefficient and pressure drop for water flow in finned tubing. The heat transfer coefficient will be determined based on multiple methods, which will allow for verification of the values obtained. With respect to the linear loss coefficient, verification of dependencies outlined in chapter 3 will be possible, as well as derivation of formulas relating to the finned tube geometry shown here. This is insightful as regards understanding flow and thermal phenomena taking place in the evaporators of modern power

boilers; moreover, it will inform the design of optimum finned tube geometry in terms of the heat transfer coefficient and linear pressure drop.

References

- [1] S. Goidich, K. Melzer, R. Roche, W. Bousquet, Innovation in supercritical boiler technology – the 270 mwe longview power project, in: PowerGen International, Orlando, Florida, USA, 2008.
- [2] S. Goidich, Technology on the march: Steady progress in supercritical once-through technology, in: COAL-GEN, Chicago, USA, 2001.
- [3] M. Krol, M. Blaszcok, Problems of determining air heater power in mechanical ventilation systems, *Rynek Energii* 107 (4) (2013) 80–84.
- [4] S. Grądziel, Nowoczesne rozwiązania konstrukcyjne kotłów energetycznych, *Piece przemysłowe & kotły VII–VIII* (2012) 24–30.
- [5] J. Taler, Procesy cieplne i przepływowe w dużych kotłach energetycznych - modelowanie i monitoring, PWN, Warszawa, 2011.
- [6] A. Błaszczuk, W. Nowak, S. Jagodzick, Effects of operating conditions on deNOx system efficiency in supercritical circulating fluidized bed boiler, *Journal of Power Technologies* 93 (1) (2013) 1–8.
- [7] [link].
URL <http://www.upsteel.com/index.php?c=index&a=show&catid=20&id=9521>
- [8] [link].
URL <http://www.metalravne.com/selector/steels/13crmo44.html>
- [9] [link].
URL <http://www.matbase.com/material-categories/metals/ferrous-metals/high-temperature-steel/material-properties-of-high-temperature-steel-13crmo-4-5.html#properties>
- [10] Allgemine Hinweise zu den Werkstoffkennwerte siehe N 604-260, EVT-Norm (1980).
- [11] G. Zdaniuk, L. Chamra, P. Mago, Experimental determination of heat transfer and friction factor in helically-finned tubes, *Experimental Thermal and Fluid Science* 32 (2008) 761–775.
- [12] R. L. Webb, R. Narayanamurthy, P. Thors, Heat transfer and friction characteristics of internal helical-rib roughness, *Transactions of the ASME: Journal of Heat Transfer* 122 (2000) 134–142.
- [13] M. Jensen, A. Vlakancic, Technical note. experimental investigation of turbulent heat transfer and fluid flow in internally finned tubes, *International Journal of Heat and Mass Transfer* 42 (1992) 1343–1351.
- [14] G. F. Hewit, Handbook of heat exchanger design, Begell House, INC., New York, 1992.

Nomenclature

\dot{q} heat flux, W/m²

c_p specific heat, J/(kgK)

d diameter, mm or m

f Fanning friction factor

f_M Moody friction factor

G mass flux, kg/(m²s)

h convective heat transfer coefficient, W/(m²K)

j Chilton-Colburn j -factor

k thermal conductivity, W/(mK)

L length, mm or m

N rib number

Nu Nusselt number

Pr Prandtl number

Re Reynolds number

St Stanton number

T temperature, °C or K

v fluid velocity, m/s